Available online at www.sciencedirect.com

SciVerse ScienceDirect

Ceramics International 38 (2012) 4541–4547

CERAMICS INTERNATIONAL

www.elsevier.com/locate/ceramint

Optimization of process conditions in casting aluminum matrix composites via interconnection of artificial neurons and progressive solutions

Mohsen Ostad Shabani, Ali Mazahery *

Hashtgerd Branch, Islamic Azad University, Hashtgerd, Iran

Received 4 January 2012; received in revised form 6 February 2012; accepted 12 February 2012
Available online 19 February 2012

Abstract

A genetic algorithm is a machine learning technique that was inspired by the analogy of biological evolution which generates solutions by repeatedly mutating and recombining parts of the best currently known solutions. In order to model and optimize the properties of A356 matrix composites, a finite element method (FEM) with artificial neural network based genetic algorithm (ANN-GA) model was developed. The tribological and mechanical properties of the aluminum matrix composite were also experimentally investigated. The results verified the accuracy of the proposed model to find the optimal process conditions in aluminum matrix composite materials.

Keywords: B. Composites; Wear; Optimal

1. Introduction

Aluminum alloys are promising structural materials due to their low density, high thermal conductivity, high specific strength and stiffness. However, their applications are restricted because of their poor wear resistance [1–3]. Wear is the process occurring at the interfaces between interacting bodies and is usually hidden from investigators by the wearing components [4–7]. However, this obstacle has been gradually overcome by scientists, revealing an intricate world of various wear modes and mechanisms. Since the early wear experiments our knowledge about wear has increased considerably and a significant progress in the description of wear mechanisms has been made. Over the past decades our views and understanding of wear have changed, including the classification of wear mechanisms. Concepts such as abrasion, adhesion and fatigue, originally used in the classification of wear mechanisms, are, now, insufficient.

Hard reinforcement phases are added to Al matrix in order to overcome the poor wear resistance and improve their high specific strength [8–10]. Particulate reinforced aluminum matrix composites are being considered for their superior mechanical and tribological properties over the conventional aluminum alloys, and therefore, these composites have gained extensive applications in automotive and aerospace industries. New materials including composite wear in a specific manner. Complex reactions and transitions often take place on the wearing surfaces and our understanding of wear mechanisms occurring is critical to the effective utilization of these materials. Characteristics of the matrix material, type, and volume fraction of reinforcements, as well as testing condition are some of the influential parameters on the wear resistance of composites.

A number of research works have been reported on dry sliding wear behavior of AMCs reinforced with various ceramic particulates [11–16]. The wear resistance of the composite was found to be considerably higher than that of the matrix alloy and increased with increasing particle content. The hard particles resist against destruction action of abrasive and protect the surface, so with increasing its content, the wear resistance enhances [17–22].

This paper aims to make an understanding of the GA optimization in process condition, mechanical and tribological behavior of A356 composite reinforced with coated B4C particulates readily accessible and relevant to industry, so that it can be brought to bear on engineering problems. A genetic algorithm operates on the basis of a population of potential solutions and it generates, over time, successive solutions by

* Corresponding author. Tel.: +98 912 563 6709; fax: +98 261 6201888.
E-mail address: chorookdyingbride@yahoo.com (A. Mazahery).

0272-8842/$36.00
doi:10.1016/j.ceramint.2012.02.031

repeatedly mutating and recombining parts of the best currently known solutions. Solutions are ranked according to a fitness function, and it is the fittest solutions that are allowed to breed. An ANN is formed by the interconnection of artificial neurons arranged in layers. The neurons are connected through links that have an associated connection weight. The ANN is then trained by a supervised learning algorithm, either the feedforward or the backpropagation learning algorithms. The former will compute the final classification results based on the connection weights regardless of whether or not the weights are optimal. The latter learning algorithm will repeatedly modify the connection weights until an optimum set of weights is found that produces the highest level of classification accuracy [23–30].

The finite element method (FEM) has undoubtedly become the most popular and powerful analytical tool for studying the behaviour of a wide range of engineering and physical problems. Several general purpose finite element softwares have been developed, verified and calibrated over the years and are now available to almost anyone who asks and pays for them. Furthermore, concepts of FEM are usually offered by all engineering departments in the form of postgraduate and even undergraduate courses. One of the important applications of FEM is the analysis of solidification problems [3,10].

A combined genetic algorithms (GA) and the artificial neural network (ANN) approach was proposed for this purpose the geometry and internal parameters of artificial neural networks (ANNs) have significant effects on the prediction performance efficiency of the network. The optimal ANN geometry is problem-dependent. Although some guidance is available in the literature for the choice of geometry and internal parameters, most networks are calibrated using the trial-and-error approach. This paper presents the use of genetic algorithms (GAs) to search the optimal geometry and values of internal parameter of a multilayer feedforward back-propagation neural network (BPNN).

Unlike most hybrid GA/ANN models which use GAs to optimize the ANN's parameters, our model emphasises the extraction of important features and utilizes the ANN to compute the fitness function of the GA [30–38].

2. Experimental procedure

The experimental process involved melting the casting Al–Si alloy in the graphite crucible using an electrical resistance furnace. Different volume fraction of coated B_4C particles were added to the melt which was raised to about 750 °C and being stirred by a graphite impeller. It was then the step cast into the CO_2-sand mould. The tension and Brinell hardness tests were used to assess the mechanical behavior of the composites. The tensile specimens were machined from composite rods according to ASTM.B 557 standard. The Brinell hardness values of the samples were measured using a ball with 2.5 mm diameter at a load of 31.25 kg.

The analysis of tribological phenomena requires, by nature, a multidisciplinary approach combining techniques derived from contact mechanics, surface physics and material and interface chemistry. As a result, there are no completely universal solutions to tribological problems. Each new case requires the very careful analysis of the specific problem under consideration in order to find the appropriate solution. Sliding is the most common tribological contact condition.

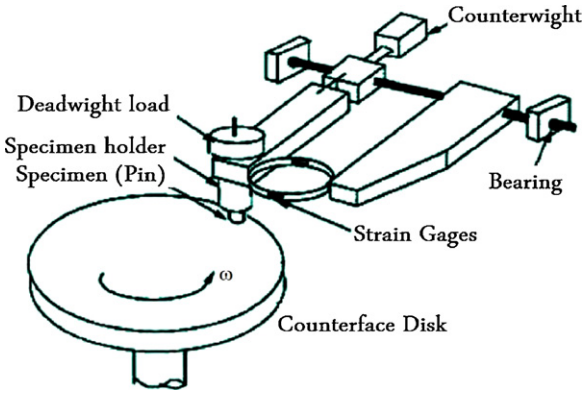

Fig. 1. Schematic diagram of the abrasion wear test.

Sliding wear tests were done under varying applied loads against case hardened steel disc of hardness 63 HRC. Test specimens were cut and shaped in the form of pins having 6 mm in diameter and 25 mm in height. Fig. 1 shows schematic diagram of the abrasion wear test.

3. Modeling

3.1. The finite element method

The finite element method is a powerful technique for solving differential or partial differential equations as well as integral equations. Any problem that can be analyzed by theoretical method can be conveniently solved by finite element (FE) method. Some factors, such as complicated geometry, anisotropy, etc., are difficult for theoretical method to treat, but are not difficult for FE method. A model-based simulation process using FEM involves doing a sequence of steps. This sequence takes two canonical configurations depending on the environment in which FEM is used. A discrete finite element model is generated from a variational or weak form of the mathematical model. This is the discretization step. The FEM equations are processed by an equation solver, which delivers a discrete solution (or solutions) [3,10,34]. The finite element analysis involves a number of steps such as finite-element discretization, generation of the element equations, assembly of element equations, imposition of boundary conditions and solution of assembled equations.

3.2. ANN

A number of fully connected three-layered feedforward networks are used comprising an input layer and a hidden layer and an output layer.

The training of networks or teaching the network to predict the parameters of interest were carried out using a non-linear neuron activation function referred as the 'sigmoidal' (in ANN

terminology) it is represented by the following function:

$$g_x = \frac{1}{2} + (1 + \tanh(x)) \quad (1)$$

For the training problem, the following parameters were found to give good performance and rapid convergence: 4 input nodes that two of them obtained from transient temperature (FEM method) namely cooling rate, temperature gradient, particles size of B_4C and volume percentage of B_4C and 4 output neurons which are porosity, hardness, UTS and weight loss. In order to find an optimal architecture, different numbers of neuron in the hidden layer were considered and root mean square (RMS) error for each network was calculated. For experiments in this paper, the total error (i.e. error based on the root mean square between the network output and target), was used as a criterion for terminating the training session [28–36].

$$RMS = \left[\frac{1}{p}\sum \left|t_j - O_j\right|^2\right]^{1/2} \quad (2)$$

Where p is the number of patterns, t_j is the target value and O_j is the actual value.

3.3. GA

3.3.1. Two-point crossover

This operator produces an offspring by crossing the chromosomes at two randomly chosen points of the two candidates (parents). The crossover operators make sure that the offspring carries genes of both parents, and in this work two-point crossover is applied using probability of unity [25,29]. In the example Table 1, the two point crossover operator is applied to two parents selected.

3.3.2. Mutation

The genes of the offspring undergo mutation with low probability in order to introduce genetic diversity to the population [36]. The gene that will be mutated is chosen using random numbers to determine its position in the chromosome. A mutated offspring is shown below as an example. In the example Table 2 the location number 4 has become loadable after applying the mutation operator.

4. Method

In order to decide whether the new set of ANNs can be included as a new member of the population in the GA, the objective function is calculated using the appropriate parameters to assess the offspring against the existing (current) population. After the evaluation of an offspring, the optimiser randomly selects a member in the population in order to compare its objective against the offspring's. If the offspring's objective is closer to the optimum the chromosome of the offspring replaces the existing member's in the population [25,29,36]. Using the random assessment technique, the population member's become fitter with evolution but at the same time the diversity of the population is maintained, which prevents premature convergence. Fig. 2 shows the flowchart of combined FEM-GA-ANN model which has been used in this investigation. The FEM method is used to calculate the transient temperature, cooling rate and temperature gradient. The combined FEM-GA-ANN model generates an initial population of A356 reinforced with coated B_4C particles from the first generation. The fitness $F(x)$ of each of the chromosome 'x' in the population is calculated and the offspring from current population using the three operators namely selection, cross-over and mutation is created. The current population is replaced with the new population. This algorithm is repeated to breed next generation. Finally, the population will move to the condition which corresponds to the best one.

Table 1
The two point crossover.

Parent 1	1	−1	1	1	1	−1	−1	−1	1	1	1
Parent 2	1	1	−1	−1	−1	1	1	1	−1	−1	1
Offspring	1	−1	1	1	−1	1	1	−1	1	1	1

Table 2
A mutated offspring.

Number	11	10	9	8	7	6	5	4	3	2	1
Old offspring	1	−1	1	1	−1	1	1	−1	1	1	1
New offspring	1	−1	1	1	−1	1	1	1	1	1	1

5. Results and discussion

An increasing amount of porosity is observed with increasing the volume fraction of composites (Fig. 3) [39–41]. The hardness of the composites increases with the volume fraction of particulates in the alloy matrix (Table 3) which is attributed to the fact that B_4C particles act as obstacles to the motion of dislocation [4,7]. The strength of the composites increases with the increase in reinforcement content (Table 3) which is due to grain refinement, the strong multidirectional stress at the A356/B_4C interface, small particle size and low degree of porosity [22].

Wear is not a material property; however, it is a complicated systems response. Thus, It must be considered in terms of a multiparameter sensitive phenomenon. 'Rolling wear', 'sliding wear', 'fretting wear' and 'impact wear' are the terms often used in practice and in literature. Sliding wear is related to asperity-to-asperity contact of the two counter surfaces, which are in relative motion against each other. Fig. 4 shows the weight loss as a function of sliding distance. It is noted that the weight loss of the composites is less than that of unreinforced alloy, increases with increase in sliding distance, and has a declining trend with increasing the particles volume fraction. In general, composites offer superior wear as compared to the alloy. This result is consistent with the rule that in general, materials with higher hardness have better wear and abrasive resistance [42,43].

Sliding wear is used to describe the type of motion which results in wear; however, it does not describe possible wear

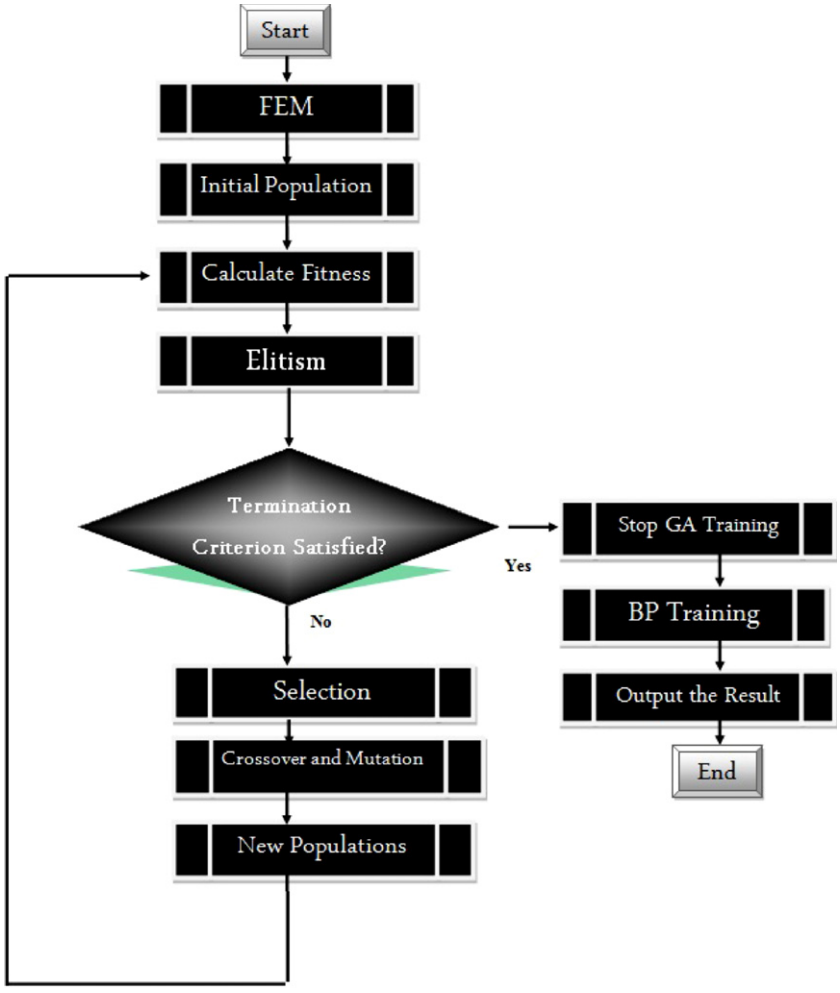

Fig. 2. Flowchart of combined FEM-GA-ANN model.

mechanisms. 'Mechanical wear', 'chemical wear' and 'thermal wear' are terms used to describe briefly wear mechanisms occurring. These descriptions of wear are necessary to characterize wear briefly; however, they are not sufficient to introduce wear models for wear rate predictions. It is usual to classify wear in terms of four different categories (traditional wear mechanisms): adhesive wear, abrasive wear, fatigue wear and tribochemical wear. Adhesive wear is characterized by the appearance of junctions between the surfaces that are subject to friction. When these junctions are weak, shear occurs at the interface of the two surfaces and there is no wear. However, when junctions are strong, the softer material is subject to shearing and, as a consequence, is transferred onto the harder material. No predictive theories have been quantitatively confirmed by experiments for the adhesive wear of ductile materials.

Abrasive wear occurs when a hard material is put into contact with a soft material. This type of wear can cause scratches, wear grooves and lead to material removal. Three-dimensional wear models of surface scratching by a hard

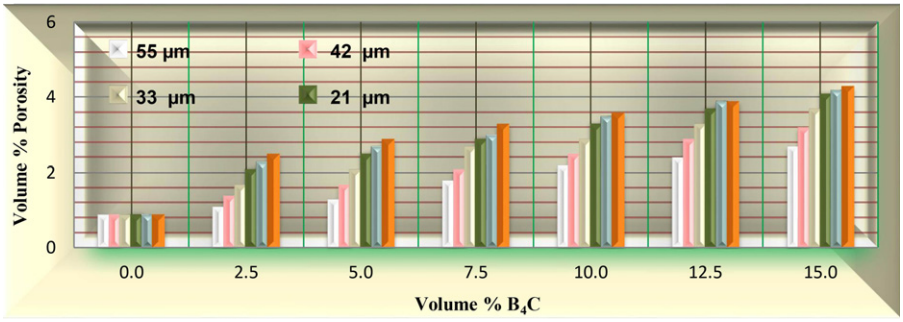

Fig. 3. Variations of porosity as a function of B_4C content.

Table 3
Hardness and UTS values versus B_4C content.

B_4C vol.%	15	12.5	10	7.5	5	2.5	0
Hardness (BHN)	82	79	77	73	71	67	64
UTS (MPa)	261	262	265	250	230	220	190

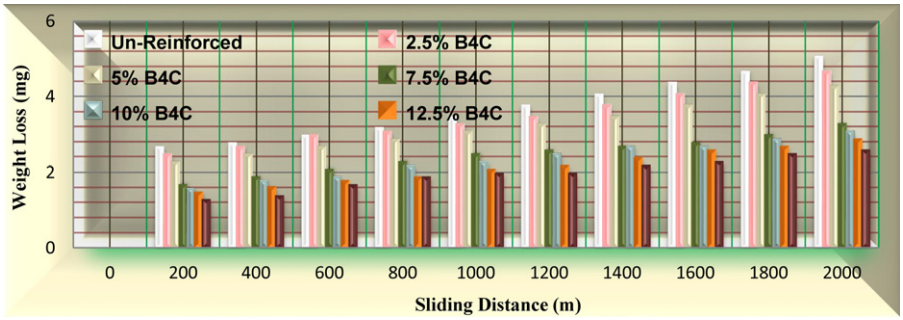

Fig. 4. Weight loss as a function of sliding distance (42 μm).

asperity have been proposed and confirmed through quantitative agreements between experimental results and theoretical predictions [14,15].

The wear volume, V, is given by the following expression:

$$V = \alpha\beta\left(\frac{WL}{H_V}\right)$$

where W is the load, L the sliding distance, α the shape factor of an asperity and β the degree of wear by abrasive asperity. Experimentally, α takes a value of about 0.1 and β varies between 0 and 1.0, depending on the value of the degree of penetration of an abrasive asperity, the shear strength at the contact interface and the mechanical properties of the wearing material.

Surface fatigue wear occurs when a material is subject to cyclical stresses. Due to strains introduced in the superficial layers of the material, cracks that are parallel to the surface develop within the material. When they reach a critical size, they generate flake-like debris. This phenomenon is also referred to as delamination wear.

Tribochemical wear is a phenomenon which involves the growth of a film of reaction products due to chemical interactions between the surfaces in contact with each other and the surrounding environment. One of the most common forms of tribochemical wear is tribooxidation wear. The increase in temperature due to friction accelerates the growth of an oxide film which detaches from the surface when it reaches a certain critical thickness. The debris thus generated can take part in the wear process or be evacuated from the friction path.

At the initial stage of sliding, the wear is mainly due to fragmentation of asperities and removal of material due to cutting and flowing actions of penetrated hard asperities into the softer surface. Higher amount of stress is expected to act on the asperities, due to the greater degree of their hardness and sharpness. Because of the higher stress concentration on these points, they get plastically deformed and some of the sharpest asperities get fractured due to combined action of normal and shear stress. During the sliding, in fact a considerable fraction of energy is spent on overcoming the frictional force, which leads to heating of the contact surfaces. Thus, it is expected that initially the temperature of the contact surface is less and hence the asperities are expected to be stronger and more rigid. As time progresses, the frictional heating increases, which leads to higher temperature and softening of the surface materials. After a certain period, because of the increase in flowability of the material on the specimen surface, slipping action is higher which results in reduction of frictional heating. The more possibility of adhesion between the counter surfaces leads to higher degree of friction [14,43].

The developed ANN consists of 4 input nodes namely cooling rate, temperature gradient, particles size of B_4C and volume percentage of B_4C. The 4 neurons in the output layer represent the 4 output parameters namely porosity, hardness, UTS and weight loss. The numbers of neurons in hidden layer are determined by trial and error during training.

The performance of the ANN depends on the network parameters such as numbers of neurons in the hidden layer,

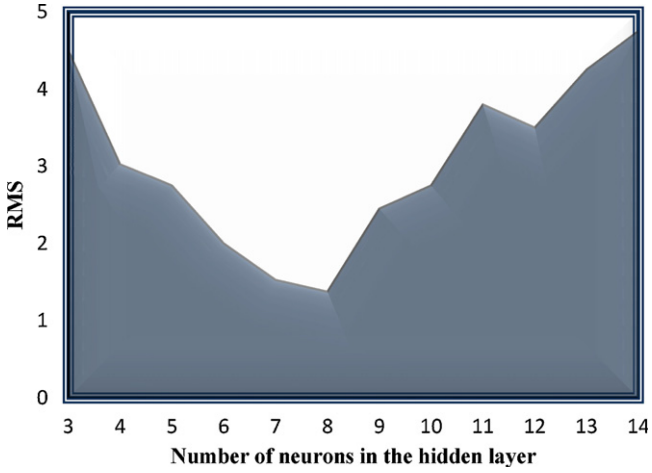

Fig. 5. The effect of numbers of neurons in the hidden layer on the network performance.

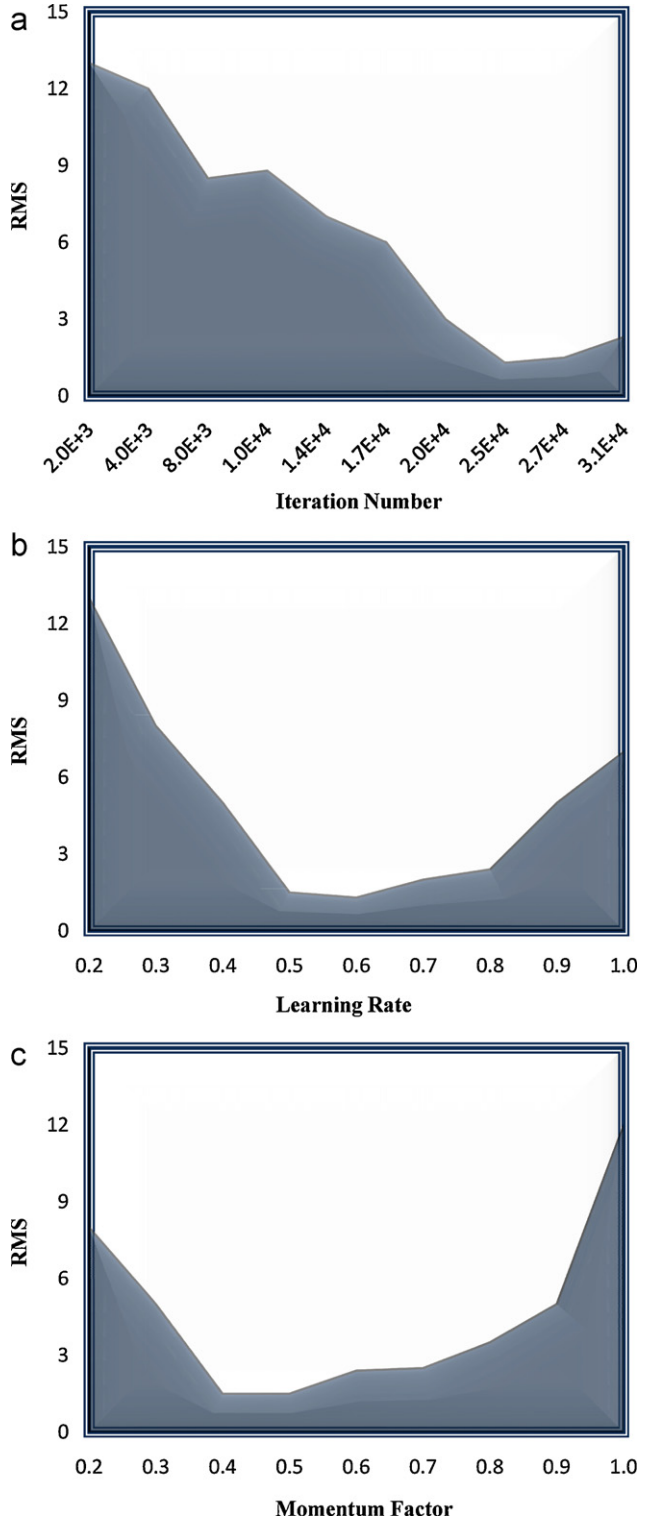

Fig. 6. The effect of a: iteration number, b: learning rate and c: momentum factor on the RMS.

momentum factor, learning rate, and iteration number [25]. The effect of numbers of neurons in the hidden layer on the network performance is shown in Fig. 5. From Fig. 5 it is clear the optimum number of neurons that gives the minimum error in the hidden layer is 8 and could be used as a fitness function in GA. Fig. 6a shows the effect of iteration number on the RMS of developed ANN. The numbers of iteration were selected from 1000 to 30,000. It is observed from this graph that the optimum number of iteration is 22,000. The probability of crossover and probability of mutation were chosen to be 0.75 and 0.07, respectively. The effects of learning rate and momentum factor on the performance of the developed ANN are shown in Fig. 6b and c. As can be seen, the optimum values of learning rate and momentum factor are 0.65 and 0.4, respectively. Final optimized A356 reinforced with coated B_4C particles process parameters are given below:

Design variables:

Volume percentage of B_4C: 11.32%
Particles size of B_4C: 36.2 μm
Cooling rate: 10 C/s
Temperature gradient: 1000 C/m

Objective functions:

Porosity: 3.34%
Hardness: 77.54 (BHN)
UTS: 264.03(MPa)
Weight loss: 2.98(mg)

Therefore, GA gives the optimal process conditions of Al matrix reinforced with B_4C particulates.

6. Conclusion

An evolutionary algorithm based on GAs has been developed for tribological and mechanical properties of fabricated A356 composite reinforced with coated B_4C particulates in stir casting. The porosity, hardness, ultimate tensile strength and weight loss of fabricated A356 composite reinforced with B_4C particulates were experimentally investigated. The prediction of ANN model was found to be in good agreement with experimental data. It is observed that FEM-ANN can be used to accelerate the optimisation process. In order to get a good accuracy, long training sessions is needed, which can be justified if this process is automated and does not require substantial analyst time.

References

[1] M.O. Shabani, A. Mazahery, Modeling of the wear behavior in A356–B4C composites, J. Mater. Sci. 46 (2011) 6700–6708.
[2] S.F. Hassan, M. Gupta, Enhancing physical and mechanical properties of Mg using nanosized Al2O3 particulates as reinforcement, Metall. Mater. Trans. A 36 (2005) 2253–2258.
[3] M.O. Shabani, A. Mazahery, The ANN application in FEM modeling of mechanical properties of Al–Si alloy, Appl. Math. Model. 35 (2011) 5707–5713.
[4] P.N. Bindumadhavan, T.K. Chia, M. Chandrasekaran, H.K. Wah, L.N. Lam, O. Prabhakar, The mechanical response of Al–Si–Mg/SiCp composite: influence of porosity, Mater. Sci. Eng. A 315 (2001) 217–226.
[5] S. Chung, B.H. Hwang, A Microstructural study of the wear behaviour of SiCp/Al composites, Tribol. Int. 27 (5) (1994) 307–314.
[6] A. Mazahery, M.O. Shabani, Study on microstructure and abrasive wear behavior of sintered Al matrix composites, Ceram. Int. (2012), doi:10.1016/j.ceramint.2012.02.008.

[7] M. Roy, B. Venkataraman, V.V. Bhanuprasad, Y.R. Mahajan, G. Sundararajan, Correlation between the characteristics of the mechanically mixed layer and wear behaviour of aluminium, Al-7075 alloy and Al-MMCs, Metall. Trans. A 23 (1992) 2833–2846.
[8] S. Skolianos, T.Z. Kattamis, Tribological properties of SiC reinforced Al-4.5% Cu-1.5% Mg alloy composites, Mater. Sci. Eng. A 163 (1993) 107–113.
[9] M.K. Surappa, S.V. Prasad, P.K. Rohatgi, Wear and abrasion of cast Al-alumina particle composites, Wear 77 (1982) 295–302.
[10] M.O. Shabani, A. Mazahery, Application of FEM and ANN in characterization of Al Matrix nano composites using various training algorithms, Metall. Mater. Trans. A (2012), doi:10.1007/s11661-011-1040-1.
[11] D.B. Miracle, S.L. Donaldson, Introduction to composites, ASM handbook, in: D.B. Miracle, S.L. Donaldson (Eds.), Composites, vol. 21, ASM International, Materials Park, 2001, pp. 3–17.
[12] T.W. Clyne, P.J. Withers, An Introduction to Metal Matrix Composites, Cambridge University Press, Cambridge, 1993Paperback Pub. in 1994 ed..
[13] T.W. Clyne, Metallic composite materials, in: R.W. Cahn, P. Haasen (Eds.), Physical Metallurgy, 4th ed., Elsevier, 1996, pp. 2568–2625.
[14] A. Mazahery, M.O. Shabani, Tribological behaviour of semisolid–semisolid compocast Al–Si matrix composites reinforced with TiB2 coated B4C particulates, Ceram. Int. (2011), doi:10.1016/j.ceramint.2011.10.016.
[15] P.N. Bindumadhavan, H.K. Wah, O. Prabhakar, Dual particle size (DPS) composites: effect on wear and mechanical properties of particulate metal matrix composites, Wear 248 (2001) 112–120.
[16] J.K.M. Kwok, S.C. Lim, High-speed tribological properties of some Al/SiCp composites: II. Wear mechanisms, Compos. Sci. Technol. 59 (1999) 55–65.
[17] S. Das, D.P. Mondal, G. Dixit, Correlation of abrasive wear with microstructure and mechanical properties of pressure die-cast aluminum hard-particle composite, Metall. Mater. Trans. A 32 (2001) 633–642.
[18] H. Ferkel, B.L. Mordike, Magnesium strengthened by SiC nanoparticles, Mater. Sci. Eng. A 298 (2001) 193–199.
[19] A. Mazahery, M.O. Shabani, Nano-sized silicon carbide reinforced commercial casting aluminum alloy matrix: experimental and novel modeling evaluation, Powder Technol. 217 (2012) 558–565.
[20] K. Akio, O. Atsushi, K. Toshiro, T. Hiroyuki, Fabrication process of metal matrix composite with nano-size SiC particle produced by vortex method, J. Jpn. Inst. Light Met. 49 (1999) 149–154.
[21] J.R. Groza, Sintering of nanocrystalline powders, Int. J. Powder Metall. 35 (1999) 59–66.
[22] H. Abdizadeh, H.R. Baharvandi, Development of high-performance A356/nano-Al2O3 composites Mater, Sci. Eng. A 518 (2009) 61–64.
[23] M.O. Shabani, A. Mazahery, Prediction of mechanical properties of cast A356 alloy as a function of microstructure and cooling rate, Arch. Metall. Mater. 56 (2011) 671–675.
[24] N. Altinkok, R. Koker, Neural network approach to prediction of bending strength and hardening behaviour of particulate reinforced (Al–Si–Mg)-aluminium matrix composites, Mater. Design 25 (2004) 595–602.
[25] V. Srinivas, K. Ramanjaneyulu, An integrated approach for optimum design of bridge decks using genetic algorithms and artificial neural networks, Adv. Eng. Softw. 38 (2007) 475–487.
[26] S.K. Singh, K. Mahesh, A.K. Gupta, Prediction of mechanical properties of extra deep drawn steel in blue brittle region using Artificial Neural Network, Mater. Design 31 (2010) 2288–2295.
[27] P.J. Lisboa, A.F.G. Taktak, The use of artificial neural networks in decision support in cancer: a systematic review, Neural Networks 19 (2006) 408–415.
[28] M.O. Shabani, A. Mazahery, Microstructural prediction of cast A356 alloy as a function of cooling rate, JOM 63 (2011) 132–316.
[29] J. Cheng, An artificial neural network based genetic algorithm for estimating the reliability of long span suspension bridges, Finite Elem. Anal. Des. 46 (2010) 658–667.
[30] R. Koker, N. Altinkok, A. Demir, Neural network based prediction of mechanical properties of particulate reinforced metal matrix composites using various training algorithms, Mater. Design 28 (2007) 616–627.
[31] A. Mazahery, M.O. Shabani, The accuracy of various training algorithms in Tribological behavior modeling of A356-B4C composites, Russ. Metall. (Metally) (2011) 699–707.
[32] Z. Sterjovski, D. Nolan, K.R. Carpenter, D.P. Dunne, J. Norrish, Artificial neural networks for modelling the mechanical properties of steels in various applications, J. Mater. Process. Technol. 170 (2005) 536–544.
[33] R. Hwang, Y. Chen, H. Huang, Artificial intelligent analyzer for mechanical properties of rolled steel bar by using neural networks, Expert Syst. Appl. 37 (2010) 3136–3139.
[34] M.O. Shabani, A. Mazahery, Artificial Intelligence in numerical modeling of nano sized ceramic particulates reinforced metal matrix composites, Appl. Math. Model. (2012), doi:10.1016/j.apm.2011.12.059.
[35] L. Fratini, G. Buffa, D. Palmeri, Using a neural network for predicting the average grain size in friction stir welding processes, Comput. Struct. 87 (2009) 1166–1174.
[36] M. Paliwal, U.A. Kumar, Neural networks and statistical techniques: a review of applications, Expert Syst. Appl. 36 (2009) 2–17.
[37] N.S. Reddy, A.K. Prasada Rao, M. Chakraborty, B.S. Murty, Prediction of grain size of Al–7Si Alloy by neural networks, Mater. Sci. Eng. A 391 (2005) 131–140.
[38] M. Tatlier, H.K. Cigizoglu, A.E. enatalar, Artificial neural network methods for the estimation of zeolite molar compositions that form from different reaction mixtures, Comput. Chem. Eng. 30 (2005) 137–146.
[39] M. Zamzam, D. Ros, J. Grosch, Fabrication of P/M in situ fiber composite materials. Part 1: formation of fibrous structure, Key Eng. Mater. 79–80 (1993) 235.
[40] W. Zhou, Z.M. Xu, Casting of SiC reinforced metal matrix composites, J. Mater. Process. Technol. 63 (1997) 358.
[41] M.O. Shabani, A. Mazahery, Prediction of wear properties in A356 matrix composite reinforced with B4C particulates, Synth. Met. 161 (2011) 1226–1231.
[42] K. Razavizadeh, T.S. Tyre, Oxidative wear of aluminium alloys, Wear 79 (1982) 325–333.
[43] S.C. Lim, M.F. Ashby, Quantitative wear maps as a visualization of wear mechanism transitions in ceramic materials, Acta Metal. 35 (1987) l–l24.